

Harmonic Behavior of Trehalose-Coated Carbon-Monoxo-Myoglobin at High Temperature

Lorenzo Cordone,* Michel Ferrand,# Eugenio Vitrano,* and Giuseppe Zaccai^{†#§}

*Dipartimento di Scienze Fisiche ed Astronomiche dell'Università di Palermo and Istituto Nazionale di Fisica della Materia, 90123 Palermo, Italy; #Institut Laue Langevin, F38042 Grenoble Cedex 9, France; and §Institut de Biologie Structurale, F-38027 Grenoble Cedex 1, France

ABSTRACT Embedding biostructures in saccharide glasses protects them against extreme dehydration and/or exposure to very high temperature. Among the saccharides, trehalose appears to be the most effective bioprotectant. In this paper we report on the low-frequency dynamics of carbon monoxo myoglobin in an extremely dry trehalose glass measured by neutron spectroscopy. Under these conditions, the mean square displacements and the density of state function are those of a harmonic solid, up to room temperature, in contrast to D₂O-hydrated myoglobin, in which a dynamical transition to a nonharmonic regime has been observed at ~180 K (Doster et al., 1989. *Nature*. 337:754–756). The protective effect of trehalose is correlated, therefore, with a trapping of the protein in a harmonic potential, even at relatively high temperature.

INTRODUCTION

Several saccharides, particularly disaccharides such as saccharose, maltose, lactose, or trehalose, are used extensively for the preservation of dry biomaterials. Embedding biological structures in glasses of these sugars avoids damage due to adverse conditions, such as dehydration and/or high temperatures. Trehalose (a disaccharide composed of two [1,1]-linked α,α units of glucopyranose) appears to be the most effective protectant in terms of functional recovery and reutilization of the biomaterial after drying (e.g., Uritani et al., 1995; Leslie et al., 1995). The preservation of dry biomaterials by sugars is a widespread phenomenon in nature. Some desert plants and animals can survive the total absence of water under a condition known as anhydrobiosis without suffering damage. Organisms in anhydrobiosis can remain without any metabolic process for several years; upon rehydration, their vegetative cycles are restarted. They exhibit extreme resistance to stress factors, and the process of complete dehydration and rehydration can be repeated several times with no apparent damage. The desert plants *Craterostigma plantagineum* and *Selaginella lepidophylla* (also called *resurrection plants*) can be heated to temperatures higher than 100°C and exposed to high vacuum when in anhydrobiosis without suffering irreversible damage. Once rehydrated, they resume their normal life cycle. A common characteristic of all organisms in anhydrobiosis is the presence of a large concentration of trehalose, which can reach 20% of their dry weight (e.g., Crowe and Crowe, 1984; Bianchi et al., 1991; Panek, 1995). This observation led to the study of the dynamics of biostructures embedded in saccharide glasses to obtain information on the effect of

sugars on internal motions that may be involved in denaturation processes. Recently, Hagen et al. (1995, 1996) and Gottfried et al. (1996) studied CO recombination after flash photolysis in carbon monoxo myoglobin (MbCO) and hemoglobin (HbCO) embedded in trehalose glasses; they reported that some part of the protein dynamics is strongly inhibited, and in particular, that the CO molecule was no longer able to leave the heme pocket, even at room temperature.

The internal dynamics of proteins is characteristically different at low and high temperatures; whereas harmonic motions dominate at low temperature (e.g., Melkers et al., 1996), additional nonharmonic contributions become relevant as the temperature increases (in myoglobin, above ~180 K). The nonharmonic motions, arising from thermal fluctuations of a protein molecule among conformational substates (Frauenfelder et al., 1988), are often called *protein-specific motions* and appear to be a prerequisite for function. Protein-specific motions have been detected in MbCO by neutron scattering (Doster et al., 1989), Mössbauer spectroscopy (Parak et al., 1982), optical absorption spectroscopy (Di Pace et al., 1992; Leone et al., 1994; Cupane et al., 1995), and molecular dynamics simulation (see e.g., Steinbach et al., 1991). In a recent paper Cordone et al. (1998) reported that the protein-specific motions, detected by Mössbauer and optical absorption spectroscopy, are significantly hindered for MbCO embedded in a trehalose glass (trehalose coated); the inhibition is much larger for the large-scale, quasidiffusive, motions detected by Mössbauer spectroscopy than for the highly localized motions, in the core of the protein, detected by optical absorption spectroscopy. We think it worthwhile to recall that the mean square fluctuations determined by Mössbauer spectroscopy are sensitive to all the motions involving the iron atom (Parak et al., 1982), whereas optical absorption spectroscopy sees only the fluctuations of the iron with respect to the heme plane (Leone et al., 1994); this makes the mean square fluctuations determined by Mössbauer spectroscopy

Received for publication 30 June 1998 and in final form 5 November 1998.

Address reprint requests to Dr. Lorenzo Cordone, Dipartimento di Scienze Fisiche ed Astronomiche, Via Archirafi 36, Università degli Studi, 90123 Palermo, Italy. Tel.: 39-91-617-1708; Fax: 39-91-616-2461; E-mail: cordone@fisica.unipa.it.

© 1999 by the Biophysical Society

0006-3495/99/02/1043/05 \$2.00

much larger than those determined by optical spectroscopy (Melkers et al., 1996).

Differences for dynamical transitions associated with motions of different localization were also observed in bacteriorhodopsin (BR), a membrane protein studied in its natural lipid environment by inelastic neutron scattering (Ferrand et al., 1993; Réat et al., 1997). Interestingly, when the membrane was dried (thus stiffening the direct protein environment), transitions at ~ 230 K and ~ 260 K already observed for certain populations of motion essentially disappeared, whereas a transition at ~ 150 K was not affected. Moreover, neutron experiments on hydrogen-deuterium-labeled BR showed that groups in the protein core were shielded from solvent effects (Réat et al., 1998); this result is in accordance with the above-mentioned Mössbauer and optical absorption spectroscopy data relative to MbCO (Cordone et al., 1998).

In MbCO, protein-specific motions involving hydrogen atoms are much less localized and of larger amplitude than protein-specific motions involving iron atoms (Melkers et al., 1996; Doster et al., 1989). To achieve a better understanding of the constraints imposed within the protein by the stiffening of the external matrix, we performed the present study on the dynamical behavior of trehalose-coated MbCO. Experiments were performed by neutron scattering, which is sensitive to the motions of the hydrogens in the picosecond to nanosecond time scale. These are homogeneously distributed over the macromolecule and sugar, and, in the frequency range examined, they reflect well the motions of the groups to which they are bound (Smith, 1991). The neutron results were compared to data discussed above from Mössbauer and optical absorption spectroscopy, with which they are complementary.

MATERIALS AND METHODS

Sample preparation

Horse myoglobin was purchased from Sigma (St. Louis, MO) and used without further purification. Trehalose was from Hayashibara Shoji (Okayama, Japan).

The protein sample was prepared by dissolving an appropriate amount of lyophilized ferric protein in a solution containing 100 mg/ml trehalose and 2×10^{-2} M phosphate buffer (pH 7, in H_2O) to give a suitable protein concentration (100 mg/ml). The solution was then equilibrated with CO and reduced by anaerobic addition of $\sim 3 \times 10^{-2}$ M sodium dithionite. Because deuterated trehalose was not available, the protein and trehalose concentrations were chosen 1) to obtain a good trehalose-protein glass and 2) to ensure that the hydrogen atoms present in the sample after desiccation were $\sim 50\%$ from the sugar and $\sim 50\%$ from the protein. Because of the sample preparation procedure, the mean square fluctuations and the density of states obtained in our measurements refer to all of the hydrogen atoms present in the sample (protein-trehalose residual bound water) and not (as when samples are in D_2O) only to the nonexchangeable hydrogens in the protein (Doster et al., 1989). An aliquot of 1 ml of the MbCO solution was spread on the internal surface of a vacuum-tight aluminum cell with a surface area of 3.6×2.9 cm². The sample was then held under a CO atmosphere during the drying process, which consisted of leaving it for 12 h in a silica gel desiccator at room temperature. The sample was then kept at 80°C under vacuum for 12 h for further dehydration and then confined under a dry nitrogen atmosphere within the aluminum cell with an

indium seal. It is important to stress that after such treatment a complete recovery of MbCO is obtained after redissolving the sample in a CO-saturated solution. A trehalose sample, otherwise identical to the previous one but not containing MbCO, was also prepared as a control. Fourier transform infrared measurements of extremely dry MbCO trehalose samples revealed the presence of traces of tightly bound water (Librizzi et al., in preparation).

Neutron scattering theory

In energy resolved incoherent neutron scattering experiments, the quantity measured is given by $S(Q, \omega, T)$, the dynamical structure factor, which is related to the neutrons scattered with a momentum transfer $\hbar Q$ and energy transfer $\hbar\omega$ at a temperature T (Marshall and Lovesey, 1971). For a harmonic system, the dynamical structure factor can be expressed in terms of atomic normal mode amplitudes and frequencies:

$$S_{\text{inc}}(\vec{Q}, \omega, T) = \sum_{L=1}^N b_{L,\text{inc}}^2 \cdot e^{-2W_L(\vec{Q})} \cdot \prod_{\lambda=1}^{3N-6} \exp\left(-\frac{n_{\lambda}\hbar\omega_{\lambda}}{2k_B T}\right) \cdot I_{n_{\lambda}}\left(\frac{\hbar|\vec{Q} \cdot \hat{c}_{\lambda}^L|^2}{2m_L\omega_{\lambda} \sinh\left(\frac{\hbar\omega_{\lambda}}{2k_B T}\right)}\right) \delta\left(\omega - \sum_{\lambda} n_{\lambda}\omega_{\lambda}\right) \quad (1)$$

where b_L is the scattering amplitude of atom L, the product is over all of the normal modes λ of frequency ω_{λ} and displacement c_L^{λ} , W_L is the Debye-Waller factor, given by

$$W_L(\vec{Q}) = \sum_{\lambda=1}^{3N-6} \left[\frac{\hbar|\vec{Q} \cdot \hat{c}_{\lambda}^L|^2}{4m_L\omega_{\lambda}} \cdot \coth\left(\frac{\hbar\omega_{\lambda}}{2k_B T}\right) \right] \quad (2)$$

In the elastic limit ($\omega = 0$) and for $Q \rightarrow 0$ (as measured on IN16; see below), the dynamical structure factor can be expressed in a Gaussian approximation (Smith, 1991):

$$\text{Limit}_{(Q \rightarrow 0)}[\ln S(Q, \omega = 0, T)] = -\langle a^2(T) \rangle Q^2 / 6 \quad (3)$$

where $\langle a^2(T) \rangle$ is the mean squared displacement over all atoms weighted by their incoherent scattering cross sections. In practice, to correct for instrument response, the intensity measured as a function of Q was normalized by its value at the lowest temperature examined (10 K). The coefficients obtained from fits of $\ln[S(Q, T)/S(Q, 10K)]$ versus Q^2 in the appropriate Q range were therefore

$$\langle u^2(T) \rangle = \langle a^2(T) \rangle - \langle a^2(10K) \rangle \quad (4)$$

For a set of quantized harmonic oscillators one has

$$\langle a^2(T) \rangle = \hbar\langle v \rangle / 2K \coth \hbar\langle v \rangle / 2k_B T \quad (5)$$

where K and $\langle v \rangle$ are the average force field constant and the average frequency of the set of oscillators considered as an Einstein solid; accordingly, the quantity $(\hbar\langle v \rangle / 2K)$ represents the zero-point mean square displacement.

The inelastic contribution (measured on IN6; see below) is related to the generalized vibrational density of states, $G(\omega)$, by

$$\text{Lim}_{Q \rightarrow 0} \left[S_{\text{inc}}(\vec{Q}, \omega, T) \frac{6\omega \left[\exp\left(\frac{\hbar\omega}{k_B T}\right) - 1 \right]}{\hbar Q^2} \right] = \sum_{L=1}^N \sum_{\lambda=1}^{3N-6} \left[\frac{b_{L,\text{inc}}^2 |\hat{c}_{\lambda}^L|^2}{m_L} \delta\left(\omega - \sum_{\lambda} n_{\lambda}\omega_{\lambda}\right) \right] = G(\omega) \quad (6)$$

The calculation of $G(\omega)$ from the measured spectra was performed by using a program by Reichardt (1984), including a correction for multiphonon terms that are not in Eq. 4 but which have been shown not to be negligible (Settles and Doster, 1997).

Neutron scattering experiments

The IN16 spectrometer at the Institut Laue Langevin (ILL), Grenoble, is a back-scattering instrument on a cold neutron guide. It was used with an incident wavelength of 6.28 Å, to which corresponds an energy resolution of ~ 1 meV and an elastic Q range of 0.43–1.93 Å⁻¹ (IN16, Yellow Book, Institut Laue Langevin, Grenoble, 1997). The instrument was used in the elastic scattering mode.

IN6 is a time-of-flight spectrometer at ILL with a time focusing feature (IN6, Yellow Book, ILL, 1997). The incident wavelength was 5.12 Å from a cold neutron guide, providing an energy resolution of 80 μeV (full width at half-maximum) and an elastic Q range of 0.2–2.0 Å⁻¹. Detectors were regrouped into banks of 0.2 Å⁻¹ resolution. IN6 was used to measure inelastic scattering on the neutron energy gain side of the spectrum to a maximum energy transfer of 25 meV. IN6 data were reduced by using the INX standard set of programs available at ILL (Rieutord, 1991). Density of state calculations were performed by using the MUPHOCOR program, which includes multiphonon corrections (Reichardt, 1984).

On both instruments, sample cells were measured inside standard ILL cryostats in the appropriate temperature range. Calibration and control procedures included the measurements of a vanadium sample, the empty cell, and transmissions.

RESULTS AND DISCUSSION

In Fig. 1 are plotted the mean square values

$$\langle x^2 \rangle = \langle u^2 \rangle / 6 = \text{Limit} (Q \rightarrow 0) \ln [S(Q, \omega = 0, T) / S(Q, \omega = 0, 10K)] \quad (7)$$

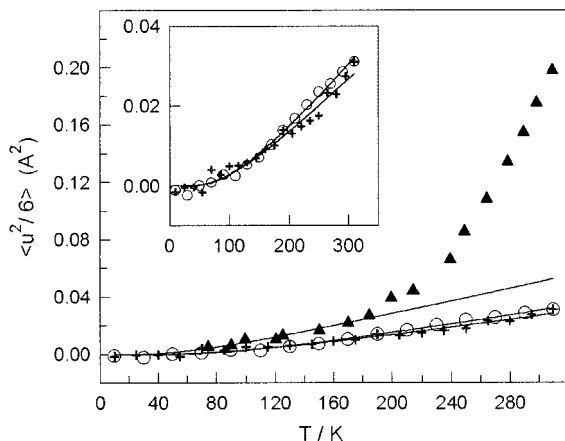


FIGURE 1 Mean squared displacements calculated from elastic neutron scattering measurements (resolution 1 meV), as described in the text, and plotted as $\langle u^2 \rangle / 6$ (Å²) versus temperature T (K), for comparison with previous data. ○, Trehalose-coated CO-myoglobin. +, Trehalose. ▲, D₂O hydrated myoglobin (data from Doster et al., 1989). The continuous lines represent the fittings of data points in terms of Eq. 8, including data from Doster et al. at low temperature (50–170 K). *Inset*: Data relative to trehalose on an expanded scale. As can be seen, the harmonic model (Eq. 8) is obeyed in the whole temperature range only for the trehalose sample, whereas nonharmonic contributions (protein-specific motions) are evident in the hydrated myoglobin sample at high temperature. (See text for detailed sample preparation.)

for trehalose-coated MbCO and trehalose alone, as a function of temperature. We also show, for comparison, the $\langle x^2 \rangle$ values reported by Doster et al. (1989) relative to nonexchangeable protons in hydrated myoglobin. Data have been normalized to give $\langle x^2(10K) \rangle = 0$.

To take quantum effects into account, data points relative to pure trehalose and trehalose-coated MbCO (Fig. 1) have been fitted in terms of the following expression for $\langle u^2(T) \rangle$ (see Eqs. 4 and 5):

$$\langle u^2(T) \rangle = \langle a^2(T) \rangle - \langle a^2(10K) \rangle = h\langle \nu \rangle / 2K \coth h\langle \nu \rangle / 2k_B T - h\langle \nu \rangle / 2K \quad (8)$$

The resulting average frequency $\langle \nu \rangle$ and amplitude of zero-point fluctuations were, respectively, $\langle \nu \rangle = 210 \pm 20$ cm⁻¹ and $[h\langle \nu \rangle / 2K]^{1/2} = 0.16 \pm 0.2$ Å.

Data in Fig. 1 show that, in contrast to hydrated proteins, the mean square displacements relative to trehalose-containing samples obey the harmonic model up to room temperature, and that there is no sizable $\langle u^2(T) \rangle$ difference between the pure trehalose and MbCO in the trehalose sample. Trehalose coating, therefore, fully hinders protein-specific motions, which are evident in hydrated protein for $T > 180$ K.

It is worth noting that the mean square displacements in trehalose-coated Mb differs from the that relative to hydrated protein reported by Doster and co-workers (1989), also in the low temperature region, where the motions are also harmonic in hydrated proteins. This differs from results obtained by Mössbauer and optical absorption spectroscopy (Cordone et al., 1998). In fact, 1) in Mössbauer experiments, data points in the harmonic regime (up to 180 K) coincided for the “trehalose-coated” and hydrated samples and 2) in optical absorption spectroscopy experiments (where information on the motions of the iron with respect to the heme plane is obtained by following the temperature dependence of the Gaussian broadening (σ^2) of the Soret band), fitting of σ^2 as a function of T yielded analogous average frequencies for myoglobin in glycerol/water solution and trehalose-coated in the low-temperature harmonic regime.

In Fig. 2 is shown the density of state functions relative to trehalose-coated MbCO and to trehalose alone at 300 K. The data show perfect Debye behavior ($G(\omega) = \text{constant} \times \omega^2$) below 10 meV, as expected for an infinite, homogeneous, harmonic solid. The low-energy transfer region is shown in the inset. Peak features at higher energy transfers (10 meV to ~ 50 meV) correspond to undamped normal modes and show some differences between the two samples. Moreover, in the low-frequency range, the 100 K (not shown) and 300 K densities of states were identical, within the limits of the poorer accuracy of the low-temperature data. This is striking behavior for a protein sample at room temperature. Indeed, the $G(\omega)$ calculated from data on myoglobin hydrated samples showed Debye behavior only at very low temperatures (Cusack and Doster, 1990). At 300 K, in such samples, it is not possible to measure meaningful $G(\omega)$ at small ω , because of strong quasielastic scattering.

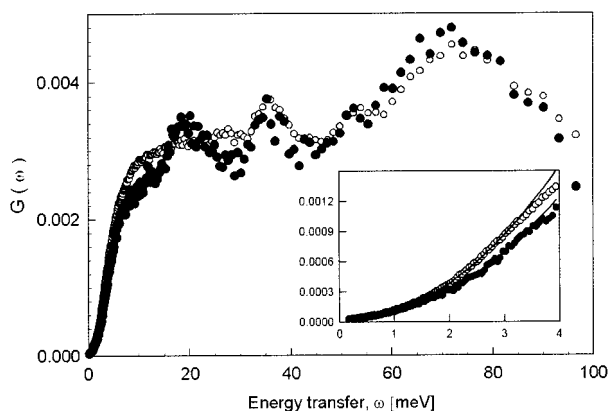


FIGURE 2 Normalized density of state functions ($G(\omega)$) versus energy transfer (ω) calculated from neutron spectroscopy measurements (resolution $80 \mu\text{eV}$) as described in the text. ●, Trehalose. ○, Trehalose-coated CO-myoglobin. *Inset*: An expansion of the low energy range (the upper curve refers to trehalose-coated CO-myoglobin). (See text for detailed sample preparation.)

At higher ω values, the $G(\omega)$ does not show the peak features seen in Fig. 2 and is interpreted in terms of damped modes. It is important to stress that, in the data reported here, all of the hydrogens in the MbCO-trehalose sample contributed to the information (exchangeable and nonexchangeable protons in the protein, sugar, and residual tightly bound water), whereas in measurements performed in D_2O hydrated myoglobin (Doster et al., 1989), only nonexchangeable hydrogens contributed to the signal (see Sample Preparation).

A comparison with optical absorption spectroscopy data, recently reported by Cordone et al. (1998), indicates that the constraints imposed by the trehalose matrix, which completely hinder the quasidiffusive motions detected by neutron scattering, have a smaller effect on the highly localized motions of the iron with respect to the heme plane. This finding is in agreement with the conclusions drawn from data on bacteriorhodopsin that the core of the protein is shielded from solvent melting (Réat et al., 1998) and with the reports by Hagen et al. (1995, 1996) and Gottfried et al. (1996) that, after flash photolysis in trehalose-coated MbCO, the diffusion of the CO molecule within the protein matrix is completely blocked, whereas geminate rebinding still shows its typical behavior.

Several disaccharides can act as bioprotectants of dry biomaterials, although they are less effective than trehalose. Analogous studies should be performed by using sugars such as saccharose, for example, for comparison with the trehalose results, to ascertain whether the blocking of protein-specific motions takes place to the same extent in these systems and to correlate the results with the ability of the protein to regain full activity after being exposed to the sugars.

In light of recent results (Librizzi et al., in preparation) indicating that traces of water are present even in extremely dry trehalose protein systems, it would be most interesting

to perform measurements analogous to those reported here in saccharide-coated proteins that have different water content and exhibit different inhibition of temperature-induced substrate interconversion.

We thank Drs. R. Carrotta, F. Librizzi, O. Comite, and C. Ebel for useful discussions and criticisms. We are very grateful to Dr. H. Schöber for help with the data analysis, as well as to ILL for financial and technical support.

This work was cofinanced by the European Community Funds for Regional Development.

REFERENCES

- Bianchi, G., A. Gamba, C. Murellie, F. Salamini, and D. Bertels. 1991. Novel carbohydrate metabolism in the resurrection plant *Craterostigma plantagineum*. *Plant J.* 1:355–359.
- Cordone, L., P. Galajda, E. Vitrano, A. Gassmann, A. Ostermann, and F. Parak. 1998. A reduction of protein specific motions in CO-ligated myoglobin embedded in a trehalose glass. *Eur. Biophys. J.* 27:173–176.
- Crowe, J. H., and L. M. Crowe. 1984. Preservation of membranes in anhydrobiotic organisms: the role of trehalose. *Science.* 223:701–703.
- Cupane, A., M. Leone, E. Vitrano, and L. Cordone. 1995. Low temperature optical absorption spectroscopy: an approach to the study of stereodynamic properties of heme proteins. *Eur. Biophys. J.* 23:385–398.
- Cusack, S., and W. Doster. 1990. Temperature dependence of the low-frequency dynamics of myoglobin. Measurement of the vibrational frequency distribution by inelastic neutron scattering. *Biophys. J.* 58:243–251.
- Di Pace, A., A. Cupane, M. Leone, E. Vitrano, and L. Cordone. 1992. Protein dynamics: vibrational coupling, spectral broadening mechanisms and anharmonicity effects in carbonmonoxy heme proteins studied by the temperature dependence of the Soret band lineshape. *Biophys. J.* 63:475–484.
- Doster, W., S. Cusack, and W. Petry. 1989. Dynamical transition of myoglobin revealed by inelastic neutron scattering. *Nature.* 337:754–756.
- Ferrand, M., A. J. Dianoux, W. Petry, and G. Zaccai. 1993. Thermal motions and function of bacteriorhodopsin in purple membranes: effects of temperature and hydration studied by neutron scattering. *Proc. Natl. Acad. Sci. USA.* 90:9668–9672.
- Frauenfelder, H., F. Parak, and R. D. Young. 1988. Conformational substates in proteins. *Annu. Rev. Biophys. Chem.* 17:451–479.
- Gottfried, D. S., E. S. Peterson, A. G. Sheikh, J. Wang, M. Yang, and J. M. Friedman. 1996. Evidence for damped hemoglobin dynamics in a room temperature trehalose glass. *J. Phys. Chem.* 100:12034–12042.
- Hagen, S. J., J. Hofrichter, and W. A. Eaton. 1995. Protein reaction kinetics in a room-temperature glass. *Science.* 269:959–962.
- Hagen, S. J., J. Hofrichter, and W. A. Eaton. 1996. Germinate rebinding and conformational dynamics of myoglobin embedded in a glass at room temperature. *J. Phys. Chem.* 100:12008–12021.
- Leone, M., A. Cupane, V. Militello, and L. Cordone. 1994. Thermal broadening of Soret band in heme complexes and in heme-proteins: role of the iron dynamics. *Eur. Biophys. J.* 23:349–352.
- Leslie, S. B., E. Israeli, B. Lighthart, J. H. Crowe, and L. M. Crowe. 1995. Trehalose and sucrose protect both membranes and proteins in intact bacteria during drying. *Appl. Environ. Microbiol.* 61:3592–3597.
- Marshall, W., and S. W. Lovesey. 1971. *Theory of Thermal Neutron Scattering*. Clarendon Press, Oxford.
- Melkers, B., E. W. Knapp, F. Parak, L. Cordone, A. Cupane, and M. Leone. 1996. Structural fluctuations of myoglobin from normal modes, Mössbauer, Raman, and absorption spectroscopy. *Biophys. J.* 70:2092–2099.
- Panek, A. D. 1995. Trehalose metabolism—new horizons in technological applications. *Braz. J. Med. Biol. Res.* 28:169–181.
- Parak, F., E. W. Knapp, and D. Kucheida. 1982. Protein dynamics. Mössbauer spectroscopy on deoxymyoglobin crystals. *J. Mol. Biol.* 161:177–194.

- Réat, V., H. Patzelt, C. Pfister, M. Ferrand, D. Oesterhelt, and G. Zaccai. 1998. Dynamics of different functional parts of bacteriorhodopsin: H-²H labelling and neutron scattering. *Proc. Natl. Acad. Sci. USA.* 95: 4970–4975.
- Réat, V., G. Zaccai, M. Ferrand, and C. Pfister. 1997. Functional dynamics in purple membrane. In *Biological Macromolecular Dynamics*. S. Cusack, H. Büttner, M. Ferrand, P. Langan, and P. Timmins, editors. Adenine Press, New York. 117–122.
- Reichardt, W. 1984. Muphacor, a Fortran program to determine the phonon density of states from neutron scattering experiments. Report no. 13.03.01P06L. Institut für Nukleare Festkörper Physik, Kernforschungszentrum, Karlsruhe GMBH, Germany.
- Rieutord, F. 1991. Institut Laue Langevin (Grenoble). Internal Report.
- Settles, M., and W. Doster. 1997. Iterative calculation of the vibrational density of states from incoherent neutron scattering data with the account of double scattering. In *Biological Macromolecular Dynamics*. S. Cusack, H. Büttner, M. Ferrand, P. Langan, and P. Timmins, editors. Adenine Press, New York. 3–8.
- Smith, J. C. 1991. Protein dynamics: comparison of simulations with inelastic neutron scattering experiments. *Q. Rev. Biophys.* 24:227–291.
- Steinbach, P. J., R. J. Loncharich, and B. R. Brooks. 1991. The effects of environments and hydration on protein dynamics: a simulation study of myoglobin. *Chem. Phys.* 158:384–394.
- Uritani, M., M. Takai, and K. Yoshinaga. 1995. Protective effect of disaccharides on restriction endonucleases during drying under vacuum. *J. Biochem.* 117:774–779.